Reduction of traffic-induced vibration of two-girder steel bridge seated on elastomeric bearings

Kim, Chul-Woo

Kawatani, Mitsuo

Hwang, Won-Sup

(Citation)
Engineering Structures,26(14):2185-2195

(Issue Date)
2004-12

(Resource Type)
journal article

(Version)
Accepted Manuscript

(URL)
https://hdl.handle.net/20.500.14094/90000470

Reduction of Traffic-Induced Vibration of Two-Girder Steel Bridge Seated on Elastomeric Bearings

Chul-Woo Kim[a*], Mitsuo Kawatani[a], Won-Sup Hwang[b]

[a] Department of Civil Engineering, Kobe University, Kobe 657-8501, Japan

[b] Department of Civil Engineering, Inha University, Incheon 402-751, Korea

Abstract

Reinforcing end-cross beam and removing bumps at expansion joints of bridges are proposed to reduce the traffic-induced vibration and to enhance the deck resistance near the expansion joint of a two-girder steel bridge with elastomeric bearings at each support. The reduction effect is investigated by means of a three-dimensional traffic-induced dynamic analysis. This study indicates that traffic-induced acceleration responses as well as dynamic reaction force of the bridge with the elastomeric bearings are greater than those of the bridge with steel pin bearings. It is observed that reinforcing the end-cross beam reduces traffic-induced vibrations regardless of bearing types, and also removing bumps is the most effective in reducing the dynamic reaction force of the bridges. Especially, for the bridge with elastomeric bearings, the maintenance of bumps near expansion joints is very important to improve not only expanding life span of the expansion joint but also the vibration serviceability of bridges.

Keywords: Traffic-induced vibration; Two-girder steel bridge; Reinforcement of end-cross beam; Removal of bumps; Elastomeric bearing; Vibration level

1. Introduction

Two-girder steel bridges with wide decks have been considered as one of the efficient types of highway bridges in Europe with the span length between 35m and 70m. The first two-girder bridges were designed and built in France in the early of 1960's. In Japan, the first two-girder steel bridge for highway is Horonai River Bridge built in 1995. Since then, two-girder steel bridges have been one of the most popular bridge types for short and medium span highway bridges in Japan. Differently from those types of bridges in Europe, highway bridges in Japan employ elastomeric bearings at the supports to minimize

* Corresponding author

Department of Civil Engineering, Kobe University, 1-1 Rokkodai, Nada, Kobe 657-8501, Japan

Phone: +81-78-803-6383; FAX: +81-78-803-6069; e-mail: cwkim@kobe-u.ac.jp

the seismic load on the bridges.

Advantages of such a simplified structural system of two-girder steel bridges include the simplicity in relation to design, fabrication, and the low cost for maintenance and construction [18]. However, the wide girder spacing and simplified lateral bracing system may cause problems related to vibration serviceability due to external dynamic loads such as wind, vehicle loads, etc.

Despite its excellence against seismic loads, Kawatani et al. [14] have reported that undesirable vertical vibration of bridges with elastomeric bearings is larger than those with the steel pin bearings under moving vehicular loadings because the elastomeric bearing works as a soft part between sub- and superstructure and allows movements in all directions by elastic displacements or rotations [22]. Yang et al. [27] and Yau et al. [28] have observed that the installation of elastic bearings can increase the dynamic response of a beam under moving train loads through a theoretical and experimental studies.

Another significant factor in the traffic-induced vibration of bridges is the impulsive dynamic wheel load caused by the vehicle passing over bumps at expansion joints. It causes severe effects on bridge members especially located near the bump, since the impulsive energy of a vehicle may be dissipated within a short period because of large damping of the vehicle. Moreover, the impulsive load at the expansion joint can also be a source to cause undesirable noises and vibrations, because supports and piers of the overhead bridge transmit the vibration to nearby buildings [4]. The undesirable vibration, so called the environmental vibration problem, has been one of major technical problems in land scarce major cities of Japan because of its high possession rates of viaducts. These environmental vibrations are usually linked with dynamic serviceability of bridges.

A number of studies on reinforcing end parts of steel bridges thus have been proposed to prevent the undesirable vibration and to enhance the resistance of expansion joints and deck slabs near the expansion joints. Chubb and Kennedy [21] observed reduction of the dynamic responses after stiffening the end-sway bracing of an existing steel bridge by field test. Yamada and Kawatani [25] investigated the effect of girder-end reinforcement on reducing traffic-induced vibration of a conventional multi-girder steel bridge under a single vehicle running by analysis, and mainly focused on the reduction effects on responses of main girders and end-sway bracings to provide a guideline for estimating sectional properties of the reinforced section, etc. However, the study failed to obtain a quantitative assessment for the vibration reduction. Moreover, the limitation of the numerical method prohibits advanced investigations considering many important factors such as the effect of bearings and profiles of bump. Nanjo et al. [19] reported that the end-cross beam reinforcement can extend life cycle of decks and expansion joints of steel girder bridges.

More detail studies have to be carried out to handle such traffic-induced vibration on the two-girder steel bridge seated on elastomeric bearings. Therefore a general procedure for the traffic-induced vibration of bridges is newly developed by means of Lagrange equation of motion, and the traffic-induced vibration analysis of a two-girder steel bridge is carried out. The natural frequencies computed from the

eigen-value analysis and analytical dynamic responses are verified through comparison with field-test data. This study examines effects of the elastomeric bearing and reinforcement of end-cross beam as well as removal of the bumps at expansion joints on the vibration of two-girder steel bridges by means of a three-dimensional traffic-induced dynamic analysis.

2. Analytical procedure

A great number of analytical studies have been devoted to the vibration of girder bridges under moving vehicles (e.g. Chompooming and Yener [2], Green and Cebon [5], Hutton and Cheung [8], Kawatani and Kim [15], Kou and DeWolf [17], Tan et al. [23], Wang et al. [24], Yang and Wu [26], Zhang et al. [29], Zhu and Law [30]).

The work reported in the current paper is based on the analytical procedure developed for analysis of girder bridges, which was validated through the comparison to the field-test data [15, 16]. It is based on the finite element method for modal analysis using three-dimensional models for both vehicle and bridge.

Two types of finite elements are adopted to idealize members of the bridge super-structure. Beam elements with six-degree-of-freedom at each node are used to idealize main girders, cross beams and guard rails of the bridge. Decks are idealized as a plate element with four nodes [1]. To improve the calculation efficiency, a process known as Guyan reduction [6] is performed. The lumped mass and Rayleigh damping are adopted to form mass and damping matrices of the bridge model, respectively. The support with elastomeric bearings is idealized by using an internal element with linear springs.

The equation of the forced vibration of a bridge system subjected to moving vehicular loadings can be defined as Eq. (1).

$$\boldsymbol{M}_b\ddot{\boldsymbol{w}}_b + \boldsymbol{C}_b\dot{\boldsymbol{w}}_b + \boldsymbol{K}_b\boldsymbol{w}_b = \boldsymbol{f}_b \tag{1}$$

where, $\boldsymbol{M}_b$, $\boldsymbol{C}_b$ and $\boldsymbol{K}_b$ indicate mass, damping and stiffness matrices of the bridge, respectively; $\boldsymbol{w}_b$ indicates displacement vector of the bridge, which can be expressed in terms of the normal coordinate q_i and mode vector ϕ_i as defined in Eq. (2); $(\cdot)$ represents the derivative with respect to time.

$$\boldsymbol{w}_b = \sum_i \phi_i q_i = \boldsymbol{\Phi} \cdot q \tag{2}$$

The load vector due to moving vehicles in Eq. (1) is defined as shown in Eq. (3).

$$\boldsymbol{f}_b = \sum_{v=1}^{nveh} \sum_{m=1}^{3} \sum_{u=1}^{2} \boldsymbol{\Psi}_{vmu}(t) P_{vmu}(t) \tag{3}$$

where, $\boldsymbol{\Psi}_{vmu}(t)$ is the distribution vector delivering wheel loads through a plate element to each node of the element; $P_{vmu}(t)$ is the vehicle wheel load as defined in Eq.(4); the subscript *v* indicates the vehicle number on the bridge; *nveh*, the total number of vehicles; the subscript *m* is the index for the axle/tire position; subscript *u*, the left and right sides of a vehicle (*u*=1, 2 indicating left and right side, respectively).

$$P_{vmu}(t)=W_{vmu}+C_{vm2u}(\dot{R}_{vm2u}-\dot{Z}_{0vmu})+K_{vm2u}(R_{vm2u}-Z_{0vmu}); \qquad m=1,2,3 \tag{4}$$

where, K_{vm2u} and C_{vm2u} are spring constant and damping coefficient of each tire, respectively; R_{vm2u}, the elastic deformation of each tire; Z_{0vmu}, the relative vertical displacement between the tire and bridge deck defined in Eq. (5) [16].

$$Z_{0vmu} = w(t, x_{vmu}) - Z_{rvmu} \tag{5}$$

where, $w(t,x_{vmu})$ is the elastic deformation of the bridge at time *t* and at the tire positioned at x_{vmu} along the direction of the wheel load; Z_{rvmu}, the pavement roughness at each axle.

The relative deformation R_{vmku} is as follows.

$$R_{vmku}=\begin{cases} Z_{v11}-(-1)^m\lambda_{xvm}\theta_{yv11}-(-1)^u(\lambda_{yv1}\theta_{xv11}-\lambda_{yv(m+1)}\theta_{xvm2})-Z_{vm2} & m=1,2;\ \ k=1;\ \ u=1,2 \\ Z_{v12}-(-1)^u\lambda_{yv2}\theta_{xv12} & m=1;\ \ k=2;\ \ u=1,2 \\ Z_{v22}+(-1)^m\lambda_{xv3}\theta_{yv2}-(-1)^u\lambda_{yv3}\theta_{xv22} & m=2,3;\ \ k=2;\ \ u=1,2 \\ 0 & otherwise \end{cases} \tag{6}$$

where, Z_{v11}, Z_{v12}, Z_{v22}, θ_{xv11}, θ_{xv12}, θ_{xv22}, θ_{yv11} and θ_{yv22} refer to the bounce of vehicle body, the parallel hop of front and rear axle respectively, the rolling of vehicle body, the axle tramp of the front and rear axles, the pitching of vehicle body and the axle windup motion of the rear axle of the vehicle model, respectively; the subscript *k* is the index for indicating vehicle body and axle (*k=1, 2* indicating vehicle body and axle, respectively).

The sign is taken to be positive if the deformation occurs in a downward direction, pitching occurs from the rear to the front axle and the rolling is generated from the right to left side.

The governing equation of a vehicle system (see Fig. 1) is derived from the energy method with Lagrange equation of motion as shown in Eq. (7) [15, 16].

$$\frac{d}{dt}\left(\frac{\partial T}{\partial \dot{a}_i}\right)-\frac{\partial T}{\partial a_i}+\frac{\partial V}{\partial a_i}+\frac{\partial U_d}{\partial \dot{a}_i}=0 \tag{7}$$

where, T is kinetic energy of the system; V, potential energy of the system; U_d, dissipation energy of the system; a_i, the *i-th* generalized co-ordinate.

$$T=\frac{1}{2}\sum_{v=1}^{nveh}\left[\sum_{k=1}^{2}\left(m_{v1k}\dot{Z}_{v1k}{}^2+J_{yvkk}\dot{\theta}_{yvkk}{}^2+J_{xv1k}\dot{\theta}_{xv1k}{}^2\right)+m_{v22}\dot{Z}_{v22}{}^2+J_{xv22}\dot{\theta}_{xv22}{}^2\right] \tag{8}$$

where, m_{v11}, m_{v12} and m_{v22} indicate the concentrated mass of the vehicle body, front and tandem axles, respectively; J_{xv11}, J_{xv12} and J_{xv22} inertia moment of vehicle body and axles around x-axis, respectively; J_{yv11} and J_{yv22} respectively inertia moment of vehicle body and tandem axle around y-axis.

$$V=\frac{1}{2}\sum_{v=1}^{nveh}\sum_{m=1}^{3}\sum_{u=1}^{2}\left[k_{vm1u}R_{vm1u}{}^2+k_{vm2u}\left(R_{vm2u}-Z_{0vmu}\right)^2\right] \tag{9}$$

$$U_d=\frac{1}{2}\sum_{v=1}^{nveh}\sum_{m=1}^{3}\sum_{u=1}^{2}\left[c_{vm1u}\dot{R}_{vm1u}{}^2+c_{vm2u}\left(\dot{R}_{vm2u}-\dot{Z}_{0vmu}\right)^2\right] \tag{10}$$

The equations of motion for the vehicle-bridge interaction are a non-stationary dynamic problem since the coefficient matrices of the equation varying to the vehicle position. An alternative step-by-step solution using Newmark's β method is applied to solve the derived system of governing equations of motion. The value of 0.25 is used for β. The solution can be obtained within the relative margin of error of less than 0.001.

The simplified algorithm is as follows;

1. Form the mass and stiffness matrices of the bridge: $\boldsymbol{M}_b$ and $\boldsymbol{K}_b$.
2. Eigen value analysis: natural frequencies and natural modes
3. Build the damping matrix of the bridge by Rayleigh damping: $\boldsymbol{C}_b$.
4. Normalize the equations of motion of the bridge.
5. Determine the longitudinal position of each tire of the vehicle on the bridge; Set initial conditions of the displacement, velocity and acceleration for each degree-of-freedom of the vehicle and bridge.
6. Start the iterative process (see Appendix A);

   Step1: Assume accelerations of the vehicle and bridge at the time $t+\Delta t$; Calculate new wheel positions of the vehicle at the time $t+\Delta t$ under the traveling speed of v; At each wheel position, the roadway profile and bridge deflection are computed; The displacement and

velocity at each mass of the vehicle model are calculated; Modal displacements and velocities of the bridge are computed

Step2: Calculate the displacements and velocities of the bridge by back transforming the modal responses in terms of a linear combination of the eigen functions; Compute the modal force of the bridge; Equations of motion of the bridge are solved to obtain the modal accelerations; Calculate the dynamic wheel load at each wheel; The equations of motion for the vehicle are solved to obtain acceleration.

Step 3: Check tolerances.

The above process from Step1 to Step3 is repeated until the tolerance is satisfied.

3. Analytical models

3.1 Bridge model

A two-span two-girder continuous steel bridge seated on elastomeric bearings is tested and analyzed. The general layout and the basic properties of the bridge are presented in Fig. 2 and Table 1 as well as Table 2, respectively. The deck slab is made of a prestressed concrete of 31cm thick, and is assumed to act compositely with main girders. Since PC decks include no cracking generally, the full concrete section of the PC deck is considered in finite element modeling.

Cross sections of the bridge before and after reinforcement are shown in Fig. 3 in which the symbols WO and WR indicate the section before and after reinforcement with 50cm thick concrete block at the end-cross beams as well as at the intermediate-cross beam on pier P1, respectively. Finite element analysis is carried out to calculate the stiffness of diaphragms; firstly the cross section with a diaphragm is idealized as a frame model, secondly a unit load/moment is loaded on the model, and lastly the displacement due to the given unit load/moment from a finite element analysis lead to the stiffness of diaphragms.

The elastomeric bearing is idealized as a spring element; the linear elastic support under a beam is considered in the analysis by simply adding the value of the spring constant to the corresponding coefficient in the diagonal of the system stiffness matrix [20].

The cross beam reinforced with concrete blocks is assumed to completely bond with deck slabs. Figure 4 illustrates the finite element model for the bridge, which consists of 231 nodes, 192 plate elements and 159 (163 for the bridge model with WR section) beam elements. The nodes V1 and V2 in Fig. 4 indicate the measured points for acceleration responses.

Fundamental natural frequencies computed from the eigen-value analysis are compared with those from field-test data as shown in Fig. 5. They are in good agreement one another and the comparison results validate the bridge model for the dynamic response analysis.

3.2 Vehicle model

The actual behavior of vehicles under varying conditions is sufficiently represented by a discrete rigid multi-body system. The vehicle is composed of the body, tires and suspension systems. Details of the vehicle idealization are shown in Fig. 1, along with the eight degrees of freedom needed to describe its movement [16]. Based on the vehicle model in Fig. 1, the bouncing motion, rolling and pitching rotations of vehicle body are considered. In addition to the motion of the vehicle body, the parallel hop and axle tramp motions of the front-axle and tandem-axle as well as the axle wind-up for the tandem-axle are taken into account in this study. Properties of the vehicle in Table 3 are measured during the on-site test at the bridge. Under analysis, the measured vehicle properties are used to compare analytical and experimental results.

3.3 Roadway surface model

Roadway surface profiles used in the dynamic analysis are obtained by Monte-Carlo simulation method based on the power spectral density (PSD) function assumed as a stationary Gaussian random process with zero mean [3]. The PSD function of the roadway surface roughness used here is expressed as in Eq. (11) [7].

$$S(\Omega) = \alpha / \left(\Omega^n + \beta^n \right) \tag{11}$$

where, $\Omega(=\omega/2\pi)$ is space frequency (cycle/m); α, β and n are roughness coefficient, shape parameter and parameter to express the distribution of the power of a given PSD curve, respectively.

As parameters of Eq. (11), α=0.001cm^2/c/m, $\beta=0.05$ and $n=2.0$, are used in this study based on the measured data from Meishin expressway in Japan (see Fig. 6). The state of roadway roughness is categorized as the road class '**A**' corresponding to a very smooth condition according to ISO 8608 based on the riding comfort of vehicles, which typically indicates a newly paved highway [12].

In the dynamic response analysis, bump profiles measured at the expansion joint near the A1 abutment under the vehicle path are considered; 16mm high and 780mm wide for the left wheel path; 14mm and 780mm in height and width for the right wheel path. To investigate the effect of bumps at an expansion joint, the roadway profile without any bump is also considered. It is worth remarking that the roadway profile used throughout the study is the sample profile which is considered in the dynamic response analysis to compare its results with field-test data.

4. Analytical results

4.1 Acceleration responses

Vertical accelerations of the bridge are estimated by superposing up to 120th modes (102.65Hz for the model before reinforcing and 106.15Hz after reinforcing), since the energy related with human perception in question is contained within the 1Hz to 80Hz band [9, 10] and useful observations have been made mainly in the frequency range between 1Hz and 100Hz. The damping constant of the bridge is assumed to have 0.7 % for the first and second modes based on field test results. The vehicle speed in the analysis and experiment was 100km/hr, and is assumed to be constant during the vehicle movement across the span.

Analytical acceleration responses and their Fourier spectra are compared with field test data to verify the validity of analytical responses. Figure 7(a) shows analytical acceleration responses and their Fourier spectra of the observation points V1 and V2 of Fig. 4. Those responses and Fourier spectra taken from the field test are shown in Fig. 7(b). The trend, wave profile and Fourier spectrum of the analytical response match well with experimental ones, although the roadway surface profile used in the analysis is an assumed one. Consequently, the quality of the agreement between the experimental and analytical results is quite acceptable in the light of potential sources of error. The dominant frequency near 3.5Hz found in the Fourier spectrum of the acceleration responses is the combined effect of the torsional and bending modes (3.37Hz) with the bouncing motion of the vehicle (3.60Hz). The dominant frequency around 18Hz may be the effect of the bending mode of deck slabs (see Fig. 5(d)).

Figure 8 shows dynamic wheel loads at the front left wheel of the tandem axle of the vehicle and vertical accelerations of decks of the pin-bearing supported bridge with end-cross beam reinforcement and bumps at expansion joints. The symbol **B** or **NB** following the WO and WR indicates the existence of the bump; **B** indicates the **B**ump at the expansion joint of A1-joint in analysis and **NB N**ot any **B**ump, respectively. The symbol PIN indicates the pin-supported bridge. The acceleration response of the deck near the A1-joint (Node11) tends to decrease after reinforcing the end-cross beam, even though no change in dynamic wheel loads is observed as shown in Figs. 8(a) and 8(b). Removal of the bump at the expansion joint (see Fig. 8(c)) diminishes both the impulsive dynamic wheel load and the peak acceleration response of the deck.

Figure 9 shows those dynamic wheel loads of the vehicle and vertical accelerations of the decks of the bridge with elastomeric bearings with the symbol ELASTO. It can be observed that the acceleration at the moment when the vehicle enters the bridge is greater than that of the pin-supported bridge because of the elastic deformation of the elastomeric bearing. The dominant acceleration response at the moment of the vehicle entering is reduced by the end-cross beam reinforcement as shown in Figs. 9(a) and 9(b).

Clearly, Figures 8 and 9 show that even the deck at the span center of the bridge supported by elastomeric bearings experiences the impulsive loading effect at the moment when the vehicle enters the bridge while the effect on the pin supported bridge is relatively very small.

4.2 Vibration Level

To assess the effect of traffic-induced vibrations on human perception, the parameter considered here is the vibration level (VL), which is expressed by Eq. (12) [13].

$$VL(\mathrm{dB}) = 20\log_{10} a / a_0 \tag{12}$$

where, a indicates the RMS value of acceleration responses revised by frequency weighting to simulate the vibration sensation of human in vertical direction, and a_0 indicates the standard acceleration defined as the least acceleration that human can perceive. It is noteworthy that a_0 is 0.001Gal in JIS C1510 [13], which differs from that defined in ISO 8041 as a_0=0.0001Gal [11].

The vibration level taken from the 1/3 octave band spectral analysis at the observation points (Node11 and Node74) is shown in Fig. 10. The vertical and horizontal scales indicate *VL* (dB) and frequency (Hz), respectively. Figure 10 shows the result that the bridge with elastomeric bearings is more sensitive to the traffic-induced vibration than the pin-supported bridge, since the vibration level of the bridge with elastomeric bearings is greater than that of the pin supported bridge. One thing worth noting here is that the countermeasure such as removing bumps as well as reinforcing the end-cross beam fails in reducing the vibration level of the member (e.g. Node74) positioned away from the bump location or the reinforced member.

Figure 11 gives a summary of the overall vibration level (OVL) with respect to each node across the span. The overall vibration level is defined as in Eq. (13).

$$OVL(\mathrm{dB}) = 10\log_{10}(10^{VL_1/10} + \cdots + 10^{VL_{21}/10}) \tag{13}$$

where, VL_1 ~ VL_{21} indicate the vibration level at the central frequencies of the 1/3 octave band frequency.

The symbol WRNB indicates the result when both reinforcement of end-cross beam and removal of bumps are considered. It can be observed from Fig. 11 that the bridge with elastomeric bearings is more easily vibrated (86dB~93dB for the section WO with bumps; 83dB~88dB for the section WR with bumps; 82dB~90dB for the section WO without bumps; 79dB~86dB for the section WR without bumps) than the bridge with steel pin bearings (78dB~86dB for the section WO with bumps; 57dB~86dB for the section WR with bumps; 72dB~86dB for the section WO without bumps; 54dB~86dB for the section WR without bumps). Certainly, the combination of reinforcing the end-cross beam and removing bumps is the most effective as expected.

An interesting fact for the bridge with elastomeric bearing is that a dominant vibration level occurs at the member near the expansion joint, while, for the bridge with steel bearing, the dominant vibration level occurs at the members near the span centre. It is by now clear that the vibration near the expansion joint can be one of sources for environmental vibrations in the two-girder steel bridges seated on elastomeric

bearings.

4.3 Reaction responses

The dynamic reaction force that usually transfers around bridges through piers and abutments is one of sources of developing undesirable vibrations of buildings nearby bridges [4]. The dynamic reaction force of bridges can be defined as a sum of static reaction due to the weight of vehicles and dynamic one generated by the inertia force of bridges and dynamic components of vehicle's wheel loads.

The reinforcement of a structural system of bridges, of course, is not an effective method to reduce the static reaction force. On the other hand, reinforcing the end-cross beam and removing bumps effectively contribute to suppress the dynamic reaction force of bridges because reinforcing the end-cross beam and removing bumps can reduce the inertia effect of bridges and the dynamic wheel load of vehicles on dynamic reactions, respectively.

Figure 12 shows the time history of the dynamic component of the reaction force at the abutment A1, in which it can be seen that the dynamic reaction when the vehicle enters the elastomeric bearing-supported bridge (t=0.5sec) is greater than that of steel pin-supported bridge. It also demonstrates, in contrast with those reduction effects on the acceleration response, that removing bumps is the most effective in reducing the dynamic reaction force of the bridges. The RMS value of dynamic components of the reaction is summarized in Fig. 13, which helps understand the fact that removing bumps is more effective in reducing the dynamic reaction force than reinforcing the end-cross beam. It is a natural consequence that the combination of two methods results in the best reduction.

5. Concluding remarks

It is observed from this study that the two-girder steel bridge with elastomeric bearings is relatively easily vibrated by moving vehicles in comparing with the bridge with steel pin bearings. Another interesting fact for the bridge with the elastomeric bearing is the occurrence of a dominant vibration level at the member near the expansion joint, while, for the bridge with steel bearing, the dominant vibration level occurs at the members near the span centre. It is clear that the vibration near the expansion joint can be one of the sources for environmental vibrations in two-girder steel bridges seated on elastomeric bearings. The end-cross beam reinforcement is one of the effective methods to curtail the impulsive response for both elastomeric bearing and pin-supported bridges. In contrast with those reduction effects on the acceleration response, removing bumps is the most effective in reducing the dynamic reaction force of the bridges. Especially, for the bridge with elastomeric bearings, the maintenance of bumps near expansion joints is very important to improve not only expanding life span of the expansion joint but also the vibration serviceability of bridges. From the observations it is sufficient to point out that the combination of reinforcing the end-cross beam reinforcement and removing bumps is the most effective.

Acknowledgements

The authors would like to thank Mr. Toshio Yasumatsu of Japan Highway Public Corporation for the use of their test data of the vehicle and bridge.

Appendix A

Iterative process by Newmark's β method:

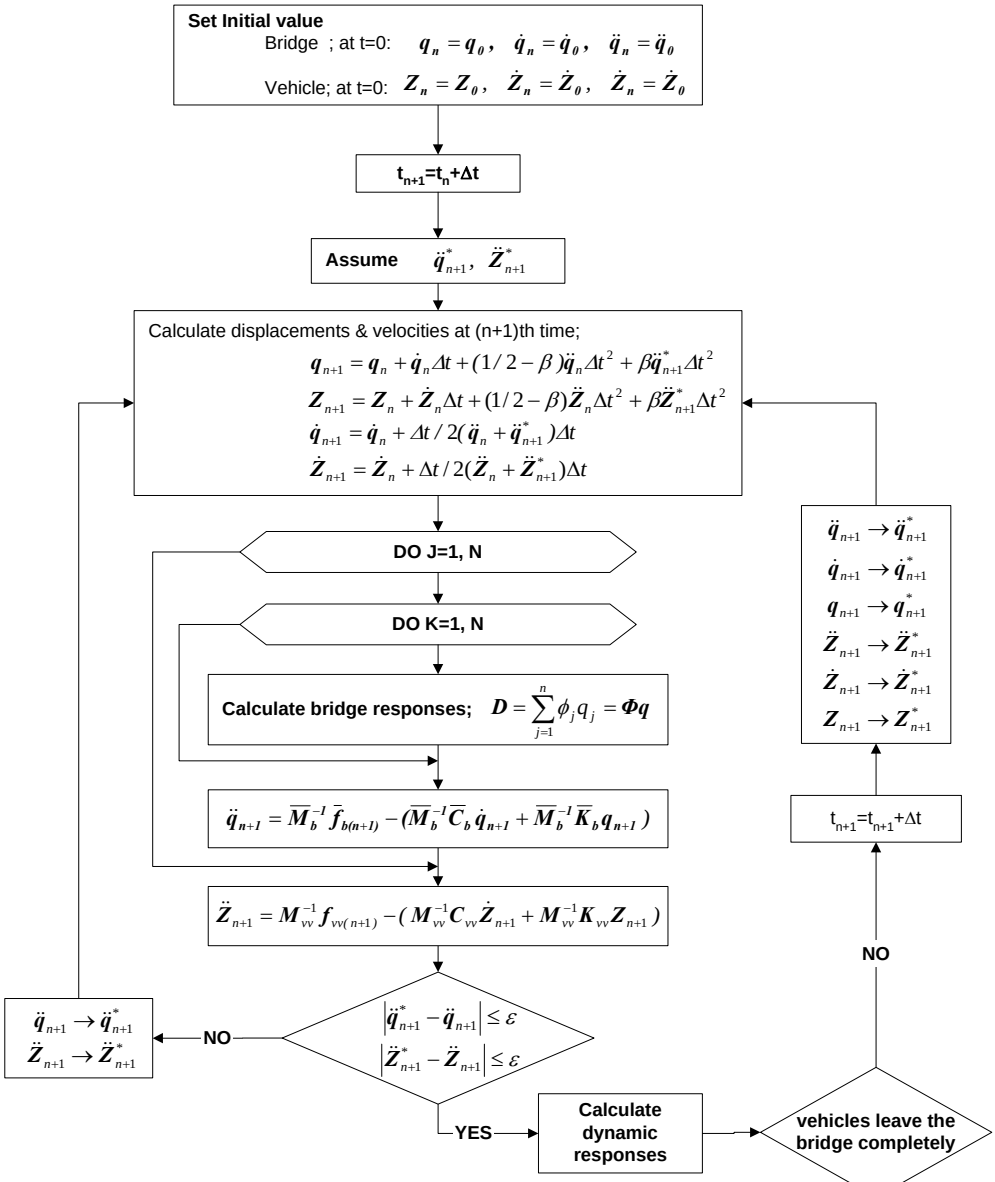

q : modal displacement of bridge
Z : displacement of vehicle
D : Displacement of bridge
N : N-th mode to be considered
$\overline{M}_b$, $\overline{C}_b$, $\overline{K}_b$: modal mass, damping and stiffness matrices of bridge
$\overline{f}_b$: modal force vector of bridge
M_{vv}, C_{vv}, K_{vv} : mass, damping and stiffness matrices of vehicle
f_{vv} : force vector of vehicle
ε : tolerance

References

[1] Bathe KJ. Finite element procedures in engineering analysis. New York: Prentice-Hall, 1982.

[2] Chompooming K, Yener M. The influence of roadway surface irregularities and vehicle deceleration on bridge dynamics using the method of lines. J Sound Vibr 1995; 183(4): 567-589.

[3] Dodds CJ, Robson MM. The description of road surface roughness. J Sound Vibr 1973; 31(2): 175-183.

[4] Fukada S, Kajikawa Y, Hayashi H, Yoshikawa M, Sanuki Y. Vibration characteristics of highway bridge with isolators and jointless system under moving vehicles. Proceedings of International Conference on Developments in Short and Medium Span Bridge Engineering '98: CSCE; 1998, CD-ROM.

[5] Green MF, Cebon D. Dynamic response of highway bridges to heavy vehicle loads: Theory and experimental validation. J Sound Vibr 1994;170(1): 51-78.

[6] Guyan RJ. Reduction of stiffness and mass matrices. AIAA J 1965; 3(2): 380.

[7] Honda H, Kajikawa Y, Kobori T. Spectra of road surface roughness on bridges. Struct Div ASCE 1982; 108(ST9): 1956-1966.

[8] Hutton SG, Cheung YK. Dynamic response of single span highway bridges. Earthquake Eng Struct Dyn 1979; 7: 543-553.

[9] ISO2631/1. Evaluation of Human Exposure to Whole-Body Vibration-Part 1: General requirements. ISO, 1985.

[10] ISO2631/2. Evaluation of Human Exposure to Whole-Body Vibration-Part 2: Continuous and shock-induced vibration in buildings (1 to 80Hz). ISO, 1985.

[11] ISO 8041. Human response to vibration – Measuring instrumentation, ISO, 1990.

[12] ISO 8608. Mechanical Vibration – Road Surface Profiles – Reporting of Measured Data. ISO, 1995.

[13] JIS C1510. Vibration level meter. Japanese Industrial Standards Committee, 1995.

[14] Kawatani M, Kobayashi Y, Kawaki H. Influence of elastomeric bearings on traffic-induced vibration of highway bridges. TRR National Research Council 2000; 2(1696): 76-82.

[15] Kawatani M, Kim CW. Computer simulation for dynamic wheel loads of heavy vehicles. Struct Eng Mech Int J 2001; 12(4): 409-428.

[16] Kim CW, Kawatani M. A comparative study on dynamic wheel loads of multi-axle vehicle and bridge responses. Proceedings of ASME International 2001 Design Engineering Technical Conferences, Symposium on Dynamics and Control of Moving Load Problems: ASME; 2001, CD-ROM.

[17] Kou JW, DeWolf JT. Vibrational behavior of continuous span highway bridge-influencing variables. J Struct Eng ASCE 1997; 123(3): 333-344.

[18] Montens M, Vollery JC, Park JH. Advantages of twin I beams composite solutions for highway and

railway bridges. Steel Structures Int J 2003; 3(1): 65-72.

[19] Nanjo A, Mori Y, Sasaki K, Sonoda K, Kiso S. Experimental study on RC end cross beams for the seismic resistance of a steel plate girder bridge. J Construction Steel JSSC 2000;8:179-186. (*in Japanese*)

[20] Paz M, Leigh W. Integrated matrix analysis of structures-theory and computation, Kluwer Academic Publishers, USA, 2001; 37

[21] Pritchard B. edited. Bridge Modification: Crossbeam replacement (by Chubb MS, Kennedy Reid IL). Thomas Telford, London, UK, 1995; 241-254.

[22] Ramberger G. Structural Bearings and Expansion Joint for Bridges. Structural Engineering Documents 6, IABSE, 2002.

[23] Tan GH, Brameld GH, Thambiratnam DP. Development of an analytical model for treating bridge-vehicle interaction. Eng Struct 1998; 20(1-2): 54-61.

[24] Wang TL, Huang D, Shahawy M, Huang K. Dynamic response of highway bridges. Comput Struct 1996; 60(6): 1021-1027.

[25] Yamada Y, Kawatani M. Analytical Study on Reduction of Traffic-Induced Vibration due to Reinforcement Procedure at Girder End. J Struct Eng JSCE 1997; 43A: 737-746. *(in Japanese)*

[26] Yang YB, Wu YS. A versatile element for analyzing vehicle-bridge interaction response. Eng Struct 2001; 23(5): 452-469.

[27] Yang YB, Lin CL, Yau JD, Chang DW. Mechanism of resonance and cancellation for train-induced vibrations on bridges with elastic bearings. . J Sound Vibr 2004;269: 345-360.

[28] Yau JD, Wu YS, Yang YB. Impact response of bridges with elastic bearings to moving loads. J Sound Vibr 2001;248(1): 9-30.

[29] Zhang QL, Vrouwenvelder A, Wardenier J. Dynamic amplification factors and EDUL of bridges under random traffic flows. Eng Struct 2001; 23(6): 663-672.

[30] Zhu XQ, Law SS. Dynamic load on continuous multi-lane bridge deck from moving vehicles. J Sound Vibr 2002; 251(4): 697-716.

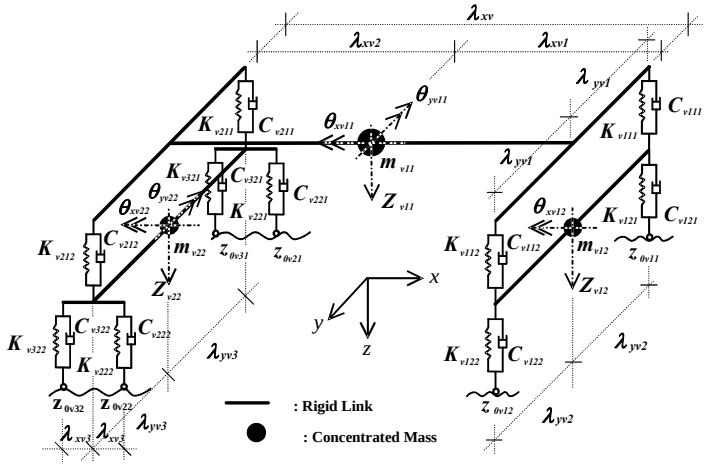

Fig. 1 Idealized vehicle model with 8DOF

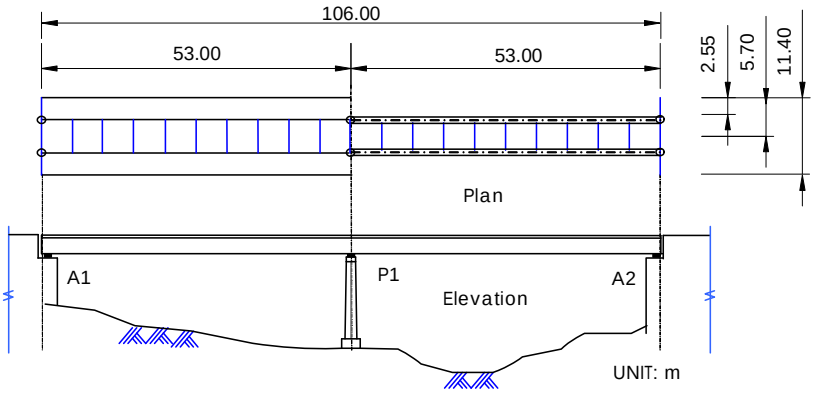

Fig. 2 General layout of two-girder bridge

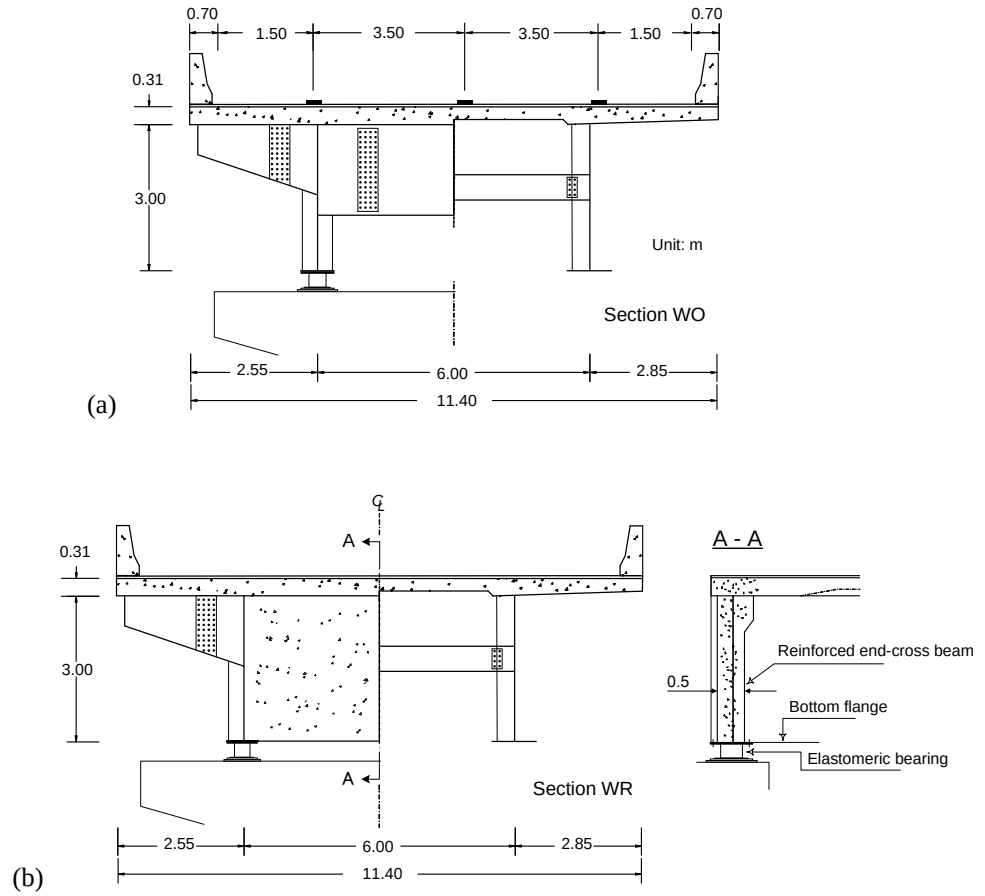

Fig. 3 Cross sections with respect to reinforcing patterns: (a) Cross section before reinforcing (Section WO); (b) Cross section after reinforcing (Section WR)

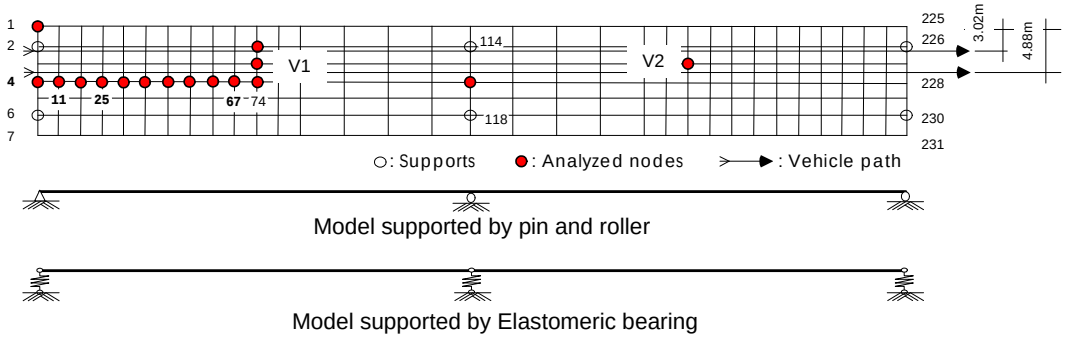

Fig. 4 Finite element model of bridge

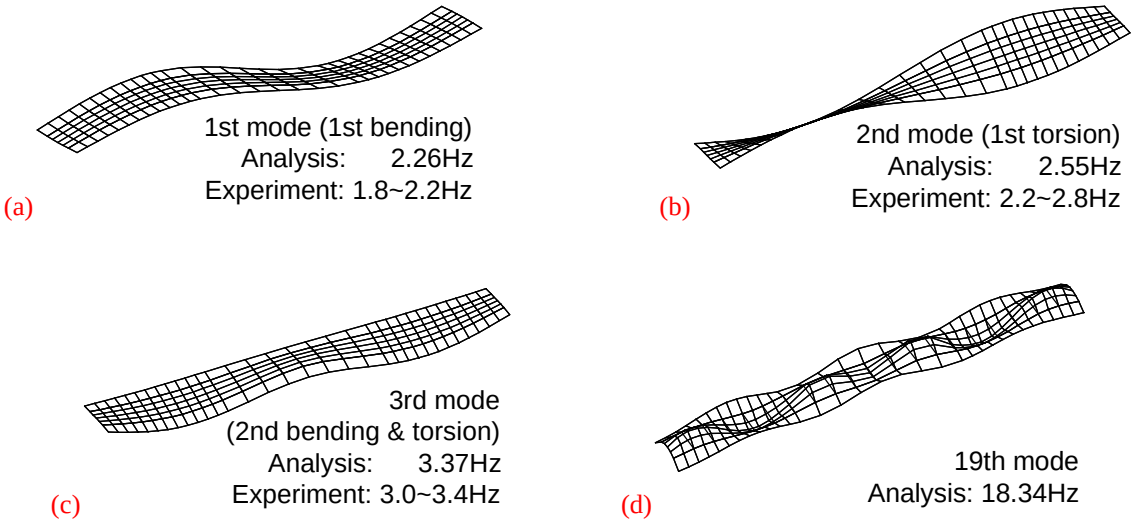

Fig. 5 Natural frequencies and mode shapes: (a) First mode in relation to bending mode of bridge; (b) Second mode in relation to torsional mode of bridge; (c) Third mode in relation to bending mode combined with torsional mode of bridge; (d) Nineteenth mode in relation to bending of deck at span center

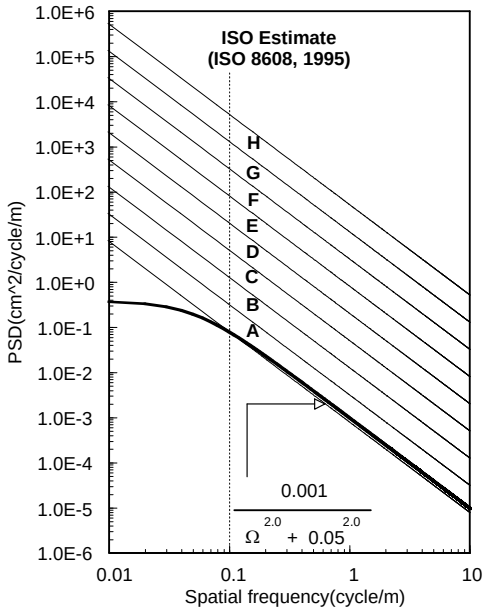

Fig. 6 PSD curve of roadway roughness

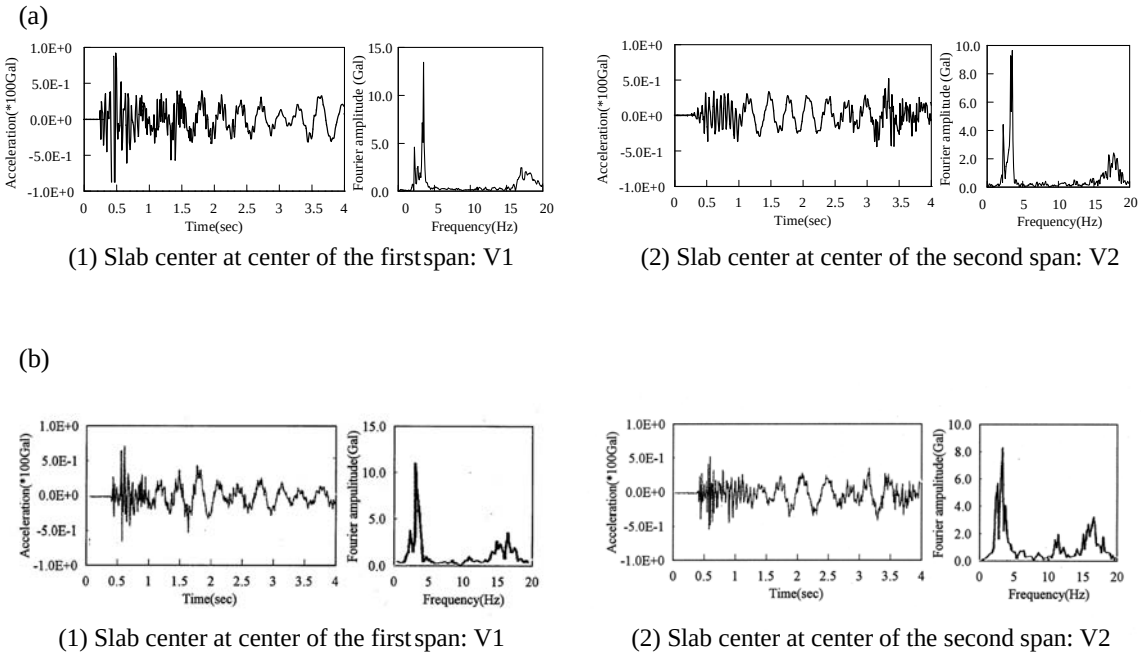

Fig. 7 Acceleration responses of bridge: a) Analysis; b) Experiment

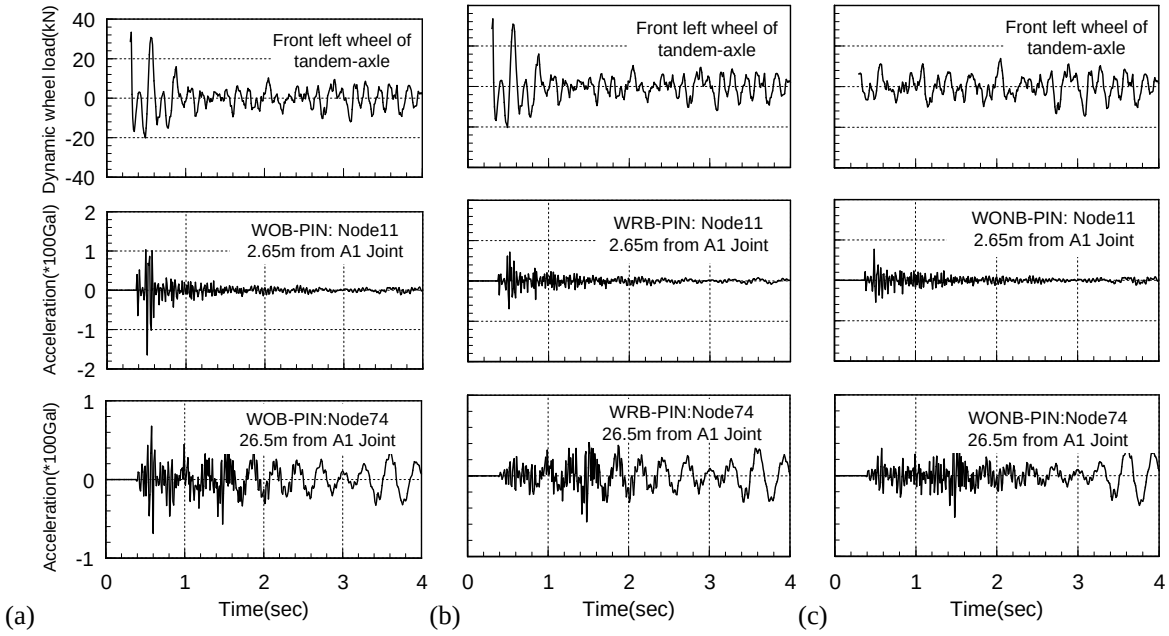

Fig. 8 Dynamic wheel load of vehicle and acceleration response of decks of bridge supported by pin bearings: (a) Without reinforcing end-cross beam and with bumps; (b) With end-cross beam reinforcement and with bumps; (c) Without reinforcing end-cross beam and without bumps

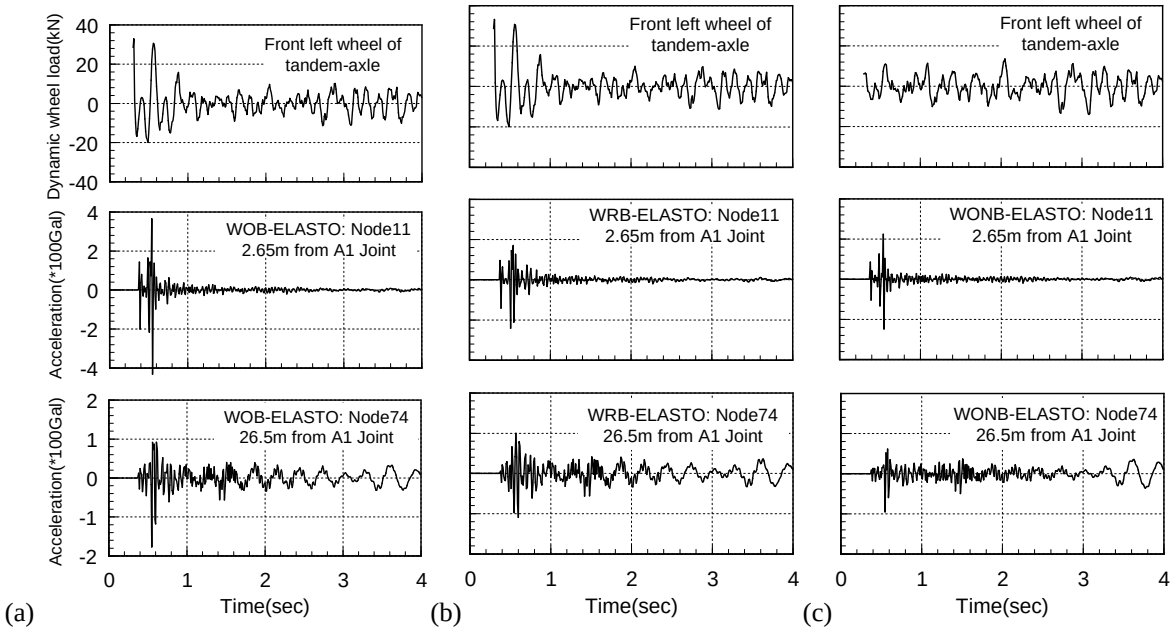

Fig. 9 Dynamic wheel load of vehicle and acceleration response of decks of bridge supported by elastomeric bearings: (a) Without reinforcing end-cross beam and with bumps; (b) With end-cross beam reinforcement and with bumps; (c) Without reinforcing end-cross beam and without bumps

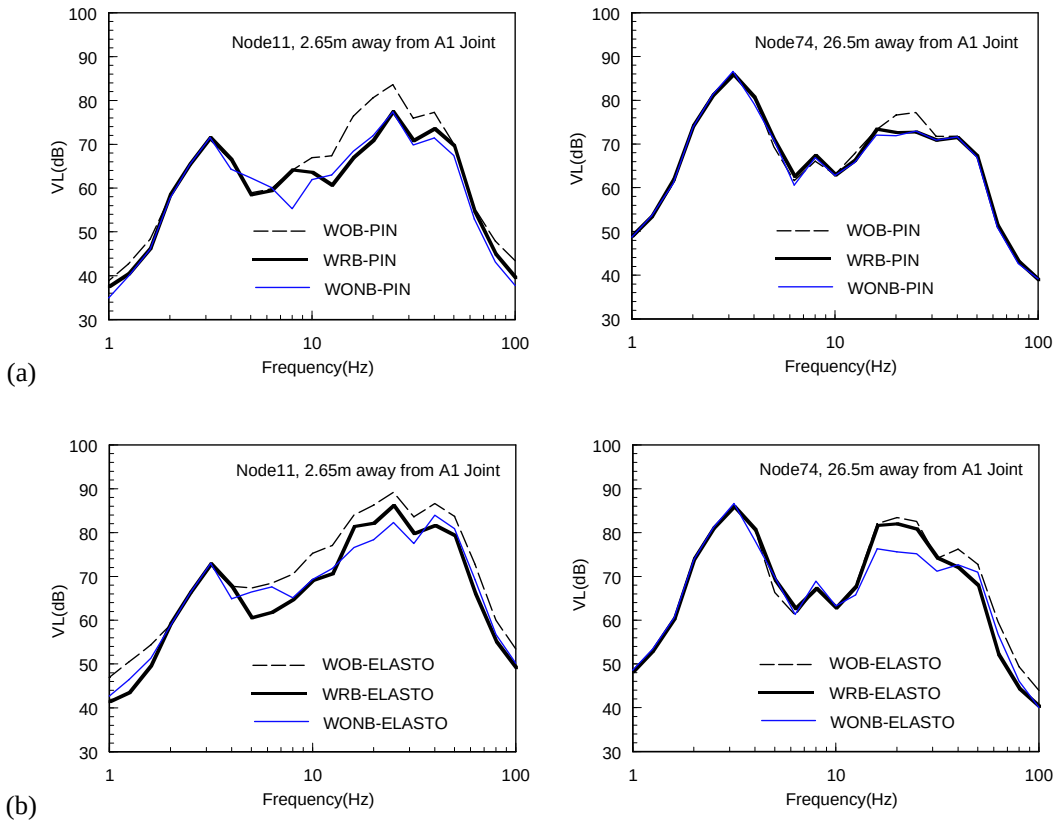

Fig. 10 1/3 octave band spectra of acceleration response: (a) Pin bearing; (b) Elastomeric bearing

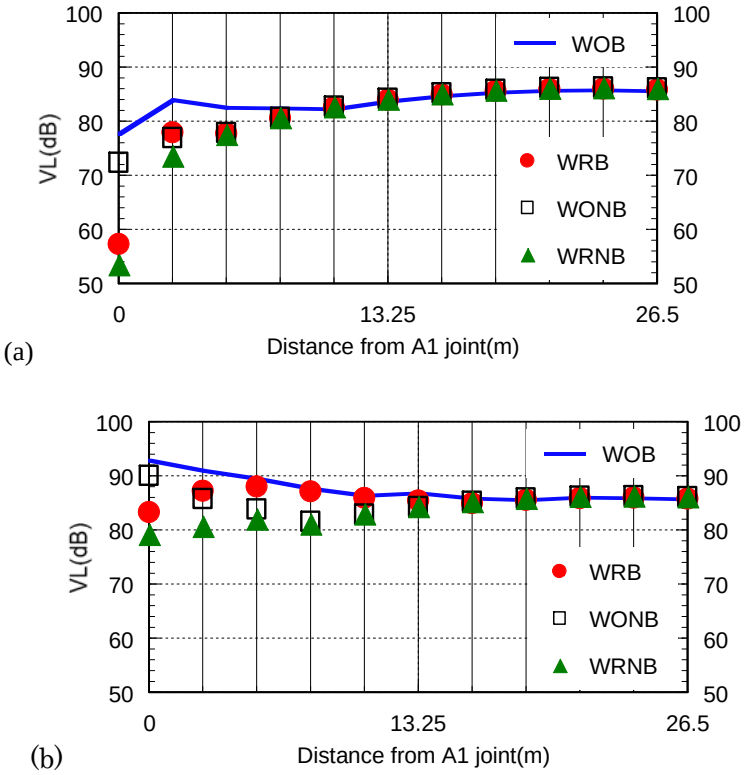

Fig. 11 Over all acceleration level with respect to countermeasures against vibration at each node of bridge: (a) Bridge with steel bearings under single vehicle running; (b) Bridge with elastomeric bearings under single vehicle running

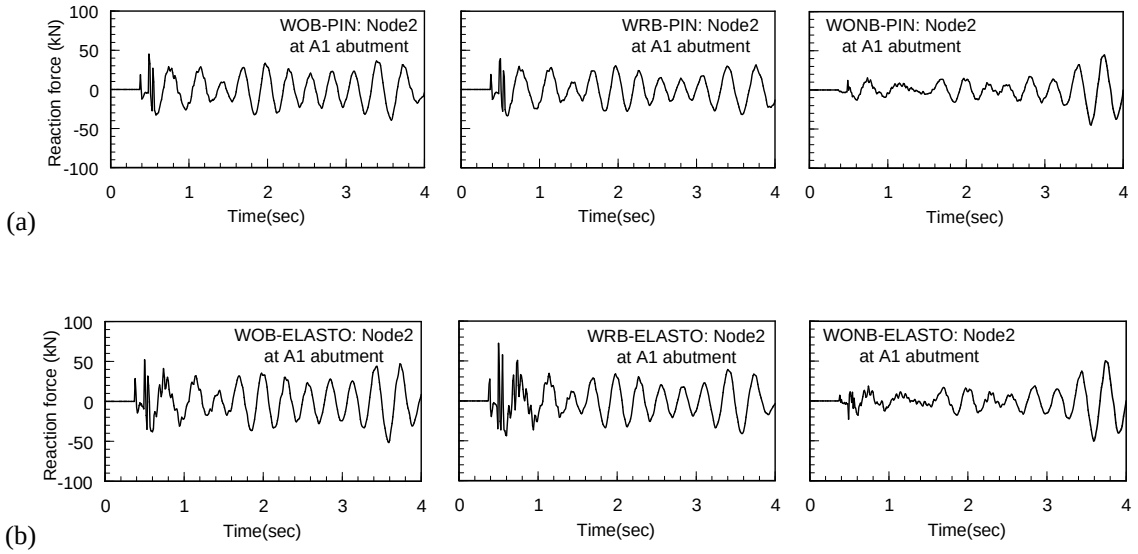

Fig. 12 Dynamic component of reaction force of bridge at A1 abutment of G1-girder: (a) Pin bearing; (b) Elastomeric bearing

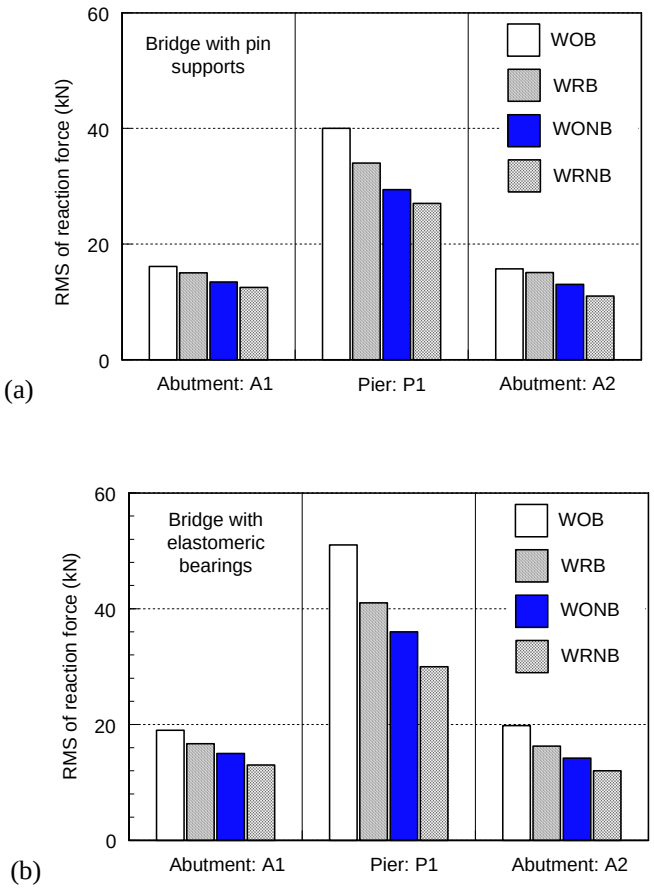

Fig. 13 RMS values of dynamic component of reaction force of bridge: (a) Pin bearing; (b) Elastomeric bearing

Table 1

Properties of bridge model

Span length (m)	53m+53m=106m
Width (m)	11.4m
Thickness of deck (cm)	31cm (45cm at bridge end)
Girder depth (m)	3m
Weight of super-structure (kN/m)	175kN/m
σ_{ck} (N/mm^2)	39.2 N/mm^2
Dimensions of the main girder (mm): at center span	WEB 3000X23 Up. FLG. 960X44 Lw. FLG. 970X40

Table 2

Spring constants of elastomeric bearing (kN/m)

	A1	P1	A2
Longitudinal	4.4718 E+02	9.8067 E+02	4.4718 E+02
Transverse	6.4332 E+02	7.3746 E+02	6.0409 E+02
Vertical	1.4834 E+06	1.0564 E+07	5.5547 E+06

Table 3

Properties of vehicle model

Total weight (KN)	Axle weight (KN)		Tread (m)	Axle distance (m)		Natural frequency (Hz)	
	Front	Rear		Front to Rear	Tandem	Pitching	Bouncing
196.03	42.95	153.08	1.86	3.86	1.30	3.19	3.60